

Prioritized Random MAC Optimization via Graph-based Analysis

Laura Toni, *Member, IEEE*, Pascal Frossard, *Senior Member, IEEE*

Abstract

Motivated by the analogy between successive interference cancellation and iterative belief-propagation on erasure channels, irregular repetition slotted ALOHA (IRSA) strategies have received a lot of attention in the design of medium access control protocols. The IRSA schemes have been mostly analyzed for theoretical scenarios for homogenous sources, where they are shown to substantially improve the system performance compared to classical slotted ALOHA protocols. In this work, we consider generic systems where sources in different importance classes compete for a common channel. We propose a new *prioritized* IRSA algorithm and derive the probability to correctly resolve collisions for data from each source class. We then make use of our theoretical analysis to formulate a new optimization problem for selecting the transmission strategies of heterogeneous sources. We optimize both the replication probability per class and the source rate per class, in such a way that the overall system utility is maximized. We then propose a heuristic-based algorithm for the selection of the transmission strategy, which is built on intrinsic characteristics of the iterative decoding methods adopted for recovering from collisions. Experimental results validate the accuracy of the theoretical study and show the gain of well-chosen prioritized transmission strategies for transmission of data from heterogeneous classes over shared wireless channels.

Index Terms

Random MAC strategies, slotted ALOHA, prioritized transmission schemes, successive interference cancellation, bipartite graphs, unequal resource allocation.

I. INTRODUCTION

In the era of Internet of the Things, the number of devices (sensors, machine terminal devices, portable devices, etc.) that are simultaneously connected to the network is expected to grow very rapidly in the near future [1], [2]. When a massive number of devices share the same channel resources, there is an obvious need for networks to be opportunistically designed with adaptive and distributed protocols. In this context, random medium access control (MAC) protocols have received a lot of attention since they do not require explicit coordination between wireless network users. At the same time, when different classes of sources compete for a common channel, as illustrated in Fig. 1, a prioritized allocation of available resources among sources is necessary in order to optimize the overall network utility. The adoption of *prioritized random* MAC strategies in future networks is thus desirable, creating the need for effective optimizations of multi-sources resource allocation strategies.

The slotted ALOHA (SA) protocol has been widely considered as one effective random MAC strategy, where users randomly select the time slots where they transmit information. If different users select the same time slot for transmission, a packet collision is experienced. While collided packets were irremediably lost in early versions of SA, recent studies have shown that collisions can be resolved by network diversity, multiuser detection, network coding strategies [3]–[5], or by successive interference cancellation (SIC) techniques [6] which substantially improves the system throughput. The key concept behind SIC is that each user might send repetitions of the same message in different slots. If two messages from two different sources are sent in the same time slot (i.e., if a collision is experienced), the base station (BS) might recover the messages through SIC if one of the collided messages has been decoded previously. The throughput gain in applying SIC to SA schemes has been initially formalized in contention resolution diversity slotted ALOHA (CRDSA), where each user sends its own message within a MAC frame and eventually a replica in a randomly selected slot [6]. If a message is correctly decoded (with no collisions), it can be used to remove the potential interference contribution caused by the replicated message. Using similar concepts, authors proposed a novel random access protocol that exploits SIC in a tree algorithm in [7]. A further analysis of such SIC-based random MAC protocol is proposed in [8].

An improvement of CRDSA has been proposed in [9], where the author introduced the optimized transmission technique for irregular repetition slotted ALOHA (IRSA) algorithm. It consists in a random SA protocol where the number of replicas that each user sends per frame (i.e., the replication rate) is not limited to two (or to any deterministic value) and it is rather randomly selected according to a pre-determined transmission probability distribution. A key connection is shown between the SIC in IRSA and the belief-propagation (BP) decoder of erasure codes on graphs [9]. This has opened the possibility of applying theory of rateless codes (and codes on graph in general) to IRSA schemes to optimize users' transmission strategies via proper selection of their transmission probability distribution [10]–[16]. For example, the IRSA has been improved with

L. Toni, and P. Frossard are with École Polytechnique Fédérale de Lausanne (EPFL), Signal Processing Laboratory - LTS4, CH-1015 Lausanne, Switzerland. Email: {laura.toni, pascal.frossard}@epfl.ch.

This work was partially funded by the Swiss National Science Foundation (SNSF) under the CHIST- ERA project CONCERT (A Context-Adaptive Content Ecosystem Under Uncertainty), project nr. FNS 20CH21 151569.

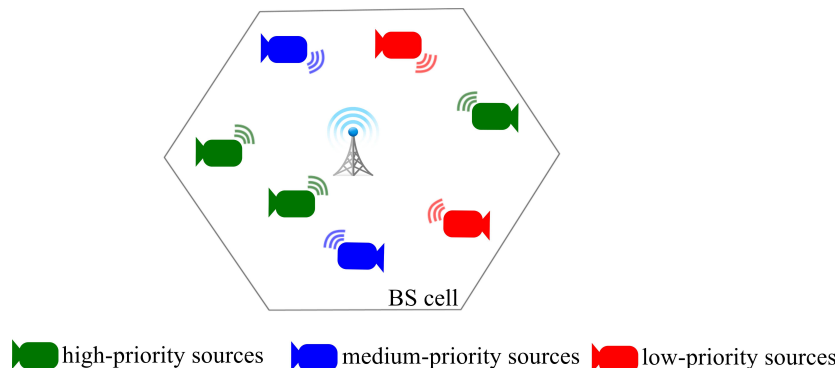


Figure 1. Scenario with multiple sources (cameras) communicating to a central base station. Different levels of priority could be given to the sources, with high- medium- and low-priority cameras, for example, which receive different shares of the network resources.

coded slotted ALOHA schemes [10], as well as frameless slotted ALOHA protocols, in which the MAC frame size is not a priori selected [11], [12]. However, to the best of our knowledge, none of the recent works on random slotted ALOHA protocols with SIC have considered unequal allocation of the channel resources among users. We exactly aim at filling this gap and extend the IRSA framework to prioritized random MAC protocols for heterogenous wireless sources.

We propose a *prioritized IRSA algorithm*, in which sources are of different classes, which transmit information to a common BS with a random IRSA strategy to access the channel. Within a MAC frame, each source randomly selects the replicas and the time slots to occupy, independently from other sources. Each prioritized source class is identified by an utility function and a transmission strategy. The utility function is a non decreasing function of the received rate and it is such that sources in higher priority classes experience a larger utility score than users in lower priority classes for a given received rate. The transmission strategy defined by the BS is characterized by the source rate and the transmission probability distribution (also defined as replication probability distribution) in IRSA, which is different in each class. The transmission probability distribution drives the replication rate of sources in each class, hence the performance of the system. Our objective is to find the best transmission strategy that maximizes the expected utility over all classes. Following the analogy between SIC and theory of codes on graph [9], we analytically derive the probability to correctly resolve collisions for data in each source class along with the expected utility per class. Our theoretical analysis studies the performance of the iterative decoding algorithms for resolving collisions in unequal transmission cases. It resembles the AND-OR tree asymptotic analysis of LDPC codes over erasure channels. We exploit intrinsic characteristics of codes on graphs codes, i.e., the convergency of the iterative decoding method, in order to derive decoding probability for random transmission probability distributions. Because of the analogy between collision recovery schemes in IRSA and iterative message-passing algorithms on graph, we note that the UEP analysis of IRSA can be linked to UEP studies for irregular LDPC codes [17]–[19]. However, there is a crucial difference between the UEP MAC strategy considered in our work and UEP rateless coding schemes. While in the latter case the code designer controls the output nodes (check nodes) rather than the input nodes (message nodes), this is exactly the opposite in the IRSA case, where the system designer controls the input nodes (source nodes) rather than the output nodes (time slot nodes). This requires a different analysis of the problem compared to [17], for example.

Our new analysis is then used to find the best unequal transmission strategy among classes in terms of both the replication probability and source rate per class, in such a way that the expected weighted utility is maximized. The underlying intuition is that more important classes should correctly receive more messages than low priority classes. This is possible either by sending more messages from high-priority classes (i.e., by tuning the resource allocation strategy) or by sending messages with a transmission rate that guarantees a lower failure probability. Results validate the accuracy of the theoretical study and show the gain of unequal transmission strategies for heterogenous classes. They also show that the proposed method perform well when compared to optimal solutions computed by simulations.

In summary, the main contributions of this work are:

- a theoretical study of the system performance in IRSA schemes with unequal transmission strategies, which leads to the asymptotic message error probability per class as well as global stability conditions;
- a new optimization problem aimed at finding the best transmission strategy in prioritized IRSA strategies, in terms of both source rate and replication probability per class, for a set of heterogenous classes;
- a solving method based on intrinsic characteristics of the iterative decoding method adopted for recovering from collisions, along with proper heuristics to derive random transmission strategies for different sources.

The reminder of this paper is organized as follows. Section II describes the scenario under consideration, together with key features of IRSA schemes. The theoretical analysis for prioritized IRSA strategies is derived in Section III, where we also provide simulation results to validate the theory. The optimization problem aimed at finding the best transmission strategy for

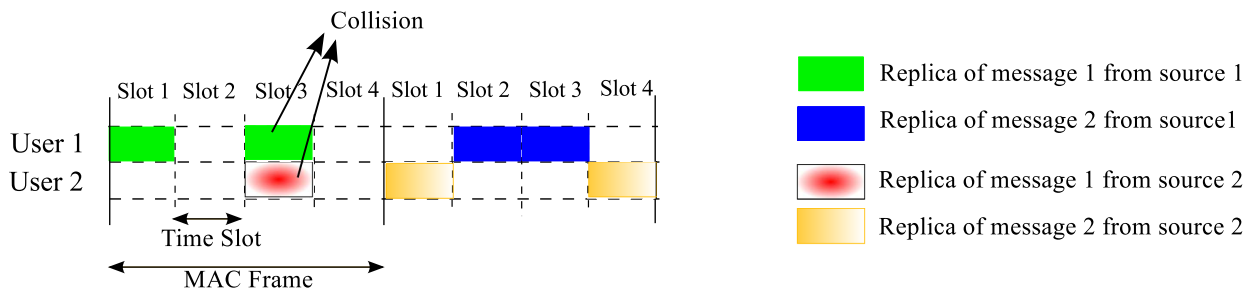


Figure 2. Example of realization of IRSA strategies for two sources and four time slots per MAC frame.

Table I
NOTATION ADOPTED IN THE PERFORMANCE ANALYSIS.

Name	Description
T_S	time slot over which a source can access the channel and send a replica message
T_{MAC}	MAC frame duration
$N = T_{MAC}/T_S$	transmission slots per MAC frame
\mathcal{C}_k	set of sources of class k
$L_k = \mathcal{C}_k $	number of sources assigned to class k
R_k	number of messages correctly received in class k
$U_k(R_k)$	utility function for class k

prioritized sources is formulated in Sec IV. The solving method and simulation results are also provided. Finally, we conclude in Section V.

II. FRAMEWORK

In the following, we first describe the system model considered in our work, then we detail key features of the SIC technique and the IRSA framework.

A. System Model

We consider M sources communicating to a common base station, that needs to decode the messages received from the sources. Sources are categorized in K priority classes and we denote by \mathcal{C}_k the set of active sources within the source class k . Let $L_k = |\mathcal{C}_k|$ be the number of sources in class k with $M = \sum_k L_k$. Without loss of generality, we assume that the source classes are sorted from the most important (\mathcal{C}_1) to the least one (\mathcal{C}_K).

We assume the time axis to be discretized in MAC frames of duration T_{MAC} and we assume that at most one source packet is sent per source within a MAC frame. This means that at most L_k messages can be sent per MAC frame from sources of class k . In our system, the sources access the channel according to the IRSA protocol [9]. Each MAC frame of duration T_{MAC} is composed of N slots of duration $T_S = T_{MAC}/N$. Each slot corresponds to a transmission interval, where one message or several interfering messages are sent. The traffic of the network is then computed as $G = M/N$. Within a MAC frame, each source transmits l replicas of one source message, as depicted in Fig. 2. Each replica is transmitted within one time slot and replicas sent from the same source are allocated to different slots, which are uniformly selected at random among the N total available slots. The replication rate l is selected by the source at random following a transmission probability distribution. We denote this distribution by $\{\Lambda_{l,k}\}_l$ for sources of class k , where $\Lambda_{l,k}$ is the probability that a source from the class k transmits l replicas within the MAC frame.

The transmission processes are handled independently by all sources. This might lead to interference on the wireless channel. We assume that if a time slot is selected only by one source, the BS correctly receives the message. When multiple sources select the same time slot for a replica transmission, a collision is experienced. The messages interfere and the information transmitted over the time slot cannot be immediately recovered. However, the receiver implements successive interference cancellation (SIC) to partially or fully resolve collisions. This is illustrated by an example in Fig. 2. In the third time slot of the first MAC frame, the message sent by source 1 (m_1) collides with the message of source 2 (m_2). This means that the BS receives message m_2 interfered by m_1 , making the messages undecodable. However, thanks to SIC techniques, the collision might be resolved. In particular, the BS can recover m_1 from the time slot 1, and once m_1 is revealed, m_2 can be “cleaned” from the interference with SIC algorithms. We assume that a perfect SIC is performed and the message is recovered with no errors [9]. In a more general scenario, this interfering-cancellation procedure is iterated and may permit the recovery of the whole set of bursts transmitted within the same MAC frame. We refer readers to [9] for a detailed description of SIC techniques applied to IRSA strategies.

Finally, we denote by $R_k \in [0, \dots, L_k]$ the number of messages from class k that are correctly received at the decoder. The reception of R_k messages leads to an utility function $U_k(R_k)$, which is a non-decreasing function of the rate. Let denote by

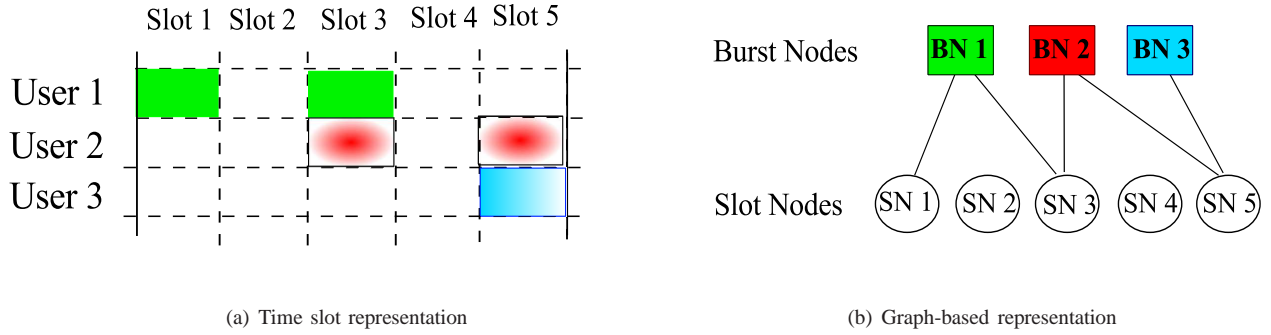


Figure 3. Example of bipartite graph associated with the IRSA scheme, with 3 sources of one message each.

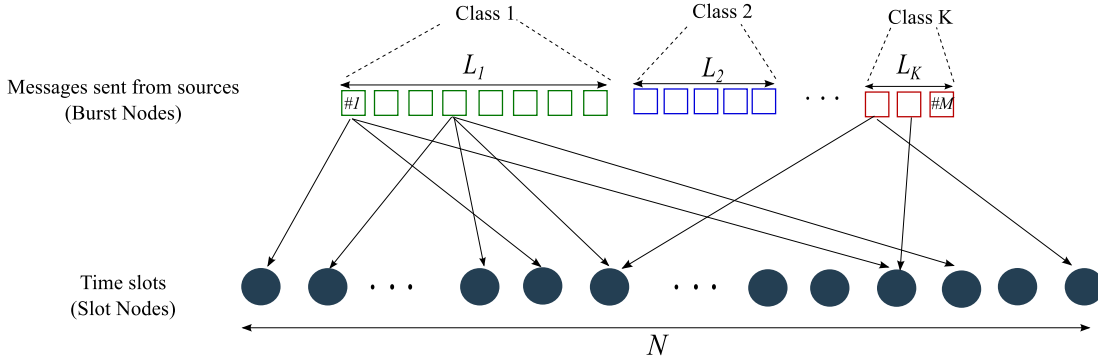


Figure 4. Graph representation for the considered MAC protocol. Sources of different classes encode the information into messages that are sent in some of the N time slots selected at random.

$\mathbf{R} = [R_1, R_2, \dots, R_K]$ the vector of received rates (or received messages) for all classes. The overall utility function for the system is given by

$$U(\mathbf{R}) = \sum_{k=1}^K w_k U_k(R_k) \quad (1)$$

where w_k is a priority score that characterizes the importance of class k , and it is such that $\sum_k w_k = 1$. Usually important classes have large weight w_k . The notation adopted in this work is summarized in Table I.

B. Graph-based representation of IRSA

To study the performance of SIC strategies applied to IRSA protocols, a graph-based representation has been introduced in [9], which shows the analogy between random MAC protocols and codes on graph. Each MAC frame can be identified by a bipartite graph where sources are represented by burst nodes (BNs), that correspond to messages, and transmission time slots are considered as slot nodes (SNs). The degree of a node defines the number of outgoing, respectively incoming edges. The probability of having a degree- l BN of class k is given by $\Lambda_{l,k}$ and the probability of having a degree- l SN is denoted by Ω_l . The degree of a BN corresponds to the repetition rate adopted by the corresponding source in the MAC frame. The degree of a SN corresponds to the number of interfering messages. Finally, the iterative message recovering procedure is associated to a message-passing algorithm along the graph. An example of the bipartite graph representation is shown in Fig. 3, where the MAC frame depicted in Fig. 3(a), characterized by 5 time slots and 3 sources with one message each, is identified by the bipartite graph in Fig. 3(b), with 5 SNs and 3 BNs.

In Fig. 4, we extend the graph-based representation to the scenario with heterogenous sources that is considered in our work. Each source in \mathcal{C}_k is identified by a BN class k , which transmits message replicas over the MAC frame independently from any other BNs. The frame status can then be represented by the bipartite graph $\mathcal{G} = (B, S, E)$ where B is the set of M burst nodes, S is the set of N SNs, and E is the set of edges. An edge (v, e) represents a transmission of BN v in the time slot e . In this case, we say that v is a neighbor of e . Recall that having a degree- l BN of class k corresponds to having a source from class k sending l message replicas within a MAC frame. Analogously, a degree- l SN reflects a time slots in which l messages have been transmitted. The transmission strategy of the IRSA can then be identified by a *node-perspective* degree distribution

with the following polynomial representations

$$\Lambda_k(x) = \sum_l \Lambda_{l,k} x^l, \quad \Omega(x) = \sum_l \Omega_l x^l \quad (2)$$

From the node-perspective degree distributions, we can also derive the *edge-perspective* degree distributions. We define $\lambda_{l,k}$ the probability for an edge to be incident to a degree- l BN of class k as follows

$$\lambda_{l,k} = \frac{l \Lambda_{l,k}}{\sum_l l \Lambda_{l,k}}. \quad (3)$$

Then, the edge-perspective degree distribution $\lambda(x)$ is given by

$$\lambda(x) = \sum_l \lambda_{l,k} x^{l-1} = \frac{\Lambda'_k(x)}{\Lambda'_k(1)} \quad (4)$$

where $\Lambda'_k(x) = d\Lambda_k(x)/dx$. Analogously, the probability of having an edge attached to a degree- l SN is

$$\rho_l = \frac{l \Omega_l}{\sum_l l \Omega_l}. \quad (5)$$

Hence, the edge-perspective degree distribution $\rho(x)$ is given by

$$\rho(x) = \sum_l \rho_l x^{l-1} = \frac{\Omega'(x)}{\Omega'(1)}. \quad (6)$$

where $\Omega'(x) = d\Omega(x)/dx$.

Different $(\Lambda_k(x), L_k)$ pairs lead to different frequency of accessing the channel and different transmission rates for the sources of class k , creating an unequal allocation of the channels among different source classes. In the following section, we show how the degree distribution is used to derive a collision recovery probability per source class, which is the probability that a message sent from a source of a given class is successively received.

III. COLLISION RESOLUTION PROBABILITY

We now evaluate the error probability for the prioritized IRSA schemes described above. The theoretical study is evaluated under the assumption of very large frame sizes ($N \rightarrow \infty$), hence the analysis presented next will refer to this asymptotic setting. The asymptotic assumption leads to theoretical analysis which is substantially simplified but yet accurate, as already proved in the literature [9], [11]. In the following, we will adopt ‘‘asymptotic setting’’ and ‘‘large network assumption’’, interchangeably.

In the following, first we derive the SN degree distribution in the case of prioritized transmission strategies. Then, to derive the decoding error probability, we extend the asymptotic analysis in [9] to the case of heterogenous sources. Finally, we provide global conditions for the stability of the iterative decoding process.

A. Node Degree Distributions

In our scenario, the base station assigns to each class k a transmission strategy, which is defined by a transmission distribution $\Lambda_k(x)$. From $\Lambda_k(x)$, the edge-perspective distribution $\lambda_k(x)$ can be evaluated as in Eq. (4). The degree distribution for the SNs, $\Omega(x)$ as well as $\rho(x)$, need to be computed. In [9], the SN-degree distribution is derived for the case in which all BNs follow the same distribution $\Lambda(x)$. Here, we extend the analysis to the case of different distributions for different classes of sources, or equivalently for different types of BNs. We denote by $P_k(n_k)$ the probability that n_k edges connect n_k BNs of class k to the same SN. This probability is given by

$$P_k(n_k) = \binom{L_k}{n_k} p_k^{n_k} (1 - p_k)^{L_k - n_k} \quad (7)$$

$$p_k = \frac{\sum_j j \Lambda_{j,k}}{N} \quad (8)$$

where p_k is the probability that a BN of class k has an edge incident to the considered SN. Note that p_k corresponds to the probability that one source from class k transmits a replica in the considered time slot. The degree distribution Ω_l for the SNs then becomes

$$\begin{aligned} \Omega_l &= \sum_{n_1, \dots, n_K: n_1 + \dots + n_K = l} P_1(n_1) P_2(n_2) \dots P_K(n_K) \\ &= \sum_{n_1, \dots, n_K: n_1 + \dots + n_K = l} \prod_k \binom{L_k}{n_k} \left(\frac{\sum_j j \Lambda_{j,k}}{N} \right)^{n_k} \left(1 - \frac{\sum_j j \Lambda_{j,k}}{N} \right)^{L_k - n_k}, \quad l = 0, \dots, M \end{aligned} \quad (9)$$

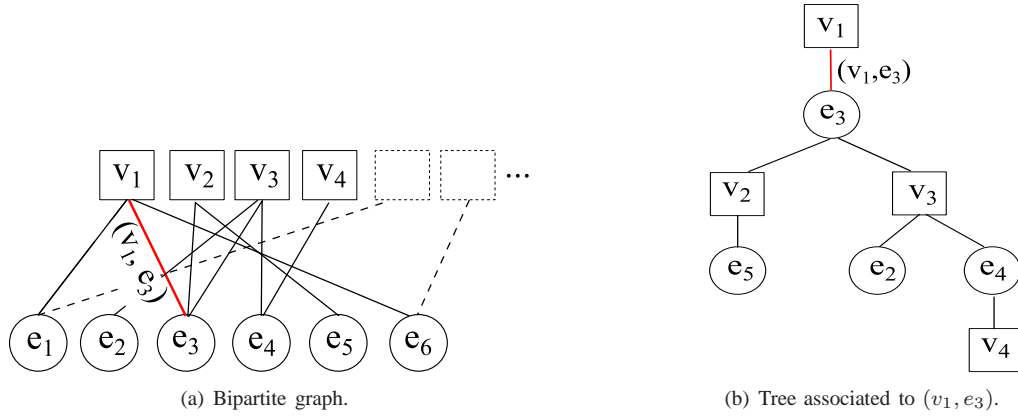


Figure 5. Example of the tree representation associated to (v_1, e_3) in the bipartite graph, assuming that the BN v_1 is of class k and it is the root of the tree $T_{i,k}$ of depth $2i = 4$.

We can simplify Eq. (9) as follows. We denote by X_i the event of having the source i transmitting in a time slot t . This event occurs with probability $p_i = (\sum_j j \Lambda_{j,k})/N$ if source i is from the class k . Since each source independently selects the time slots for transmission, we have that X_1, X_2, \dots, X_M are independent Bernoulli processes, each one with its own probability of success p_i . Then $\Omega_l = P(S_M = l)$ can be modeled as a Poisson binomial process [20], where $S_M = X_1 + X_2 + \dots + X_M$ is the sum of the considered events (i.e., S_M sources transmitting in the time slot t). This permits to express Eq. (9) as

$$\Omega_l = \sum_{A \in \mathcal{F}_l} \prod_{i \in A} (1 - p_i) \prod_{i \in A^c} p_i \quad (10)$$

where \mathcal{F}_l is the set of all subsets of l integers that can be selected in M , A is one of these possible subsets, and A^c is the complement of A , given by $\{1, 2, \dots, M\} \setminus A$. From [21], [22], the above expression becomes

$$\begin{aligned} \Omega_l &= \frac{1}{M+1} \left\{ \sum_{j=1}^M C^{-jl} \left[\prod_{m=1}^M (1 + (C^j - 1)p_m) \right] \right\} \\ &= \frac{1}{M+1} \left\{ \sum_{j=1}^M C^{-jl} \left[\prod_{k=1}^K (1 + (C^j - 1)p_k)^{L_k} \right] \right\} \end{aligned} \quad (11)$$

where $C = \exp[2\pi i/(M+1)]$, with $i = \sqrt{-1}$. The last equality follows from the fact that sources from the same class have the same probability of success p_k . Finally, for large M and small p_i 's, Ω_l can be approximated by a Poisson process [23]

$$\Omega_l \approx \frac{\left(\sum_{m=1}^M p_m \right)^l \exp\left(-\sum_{m=1}^M p_m\right)}{l!} = \frac{\left(\sum_{k=1}^K L_k p_k \right)^l \exp\left(-\sum_{k=1}^K L_k p_k\right)}{l!} \quad (12)$$

Note that we are considering large frame size networks ($N \rightarrow \infty$), which leads also to large M values. Finally, each p_i is inversely proportional to N and it becomes small for large MAC frame size (i.e., large N). This then justifies the assumptions considered to derive the above approximation.

We can then derive the node degree distribution for SNs as

$$\Omega(x) = \sum_{l=1}^M \Omega_l x^l \approx \exp(-\chi) \sum_{l=1}^M \frac{(\chi x)^l}{l!} \quad (13)$$

where $\chi = \sum_{k=1}^K L_k p_k$. Under the assumption of large networks, Eq. (13) can be further simplified as $\Omega(x) \approx \exp(-\chi(1-x))$. Finally, from Eq. (6), the edge-perspective degree distribution for a SN becomes

$$\rho(x) = \frac{\Omega'(x)}{\Omega'(1)} = \exp(-\chi(1-x)) = \exp\left(-G \sum_k \frac{\Lambda'_k(1)}{\sum_k L_k} (1-x)\right) \quad (14)$$

where $G = \sum_k L_k/N$ is the traffic of the network.

B. Collision Recovery Probability

We now study the collision recovery probability and analyze the asymptotic behavior of the message-passing algorithm used in the SIC method. We extend the analysis in [9] and consider the case of prioritized transmission strategies. The analysis considers the AND-OR tree asymptotic analysis, which is frequently used in evaluating rateless codes performance [24], [25] and it has been already introduced for IRSA strategies [9], [11].

First, we show the dependency among the nodes in the SIC algorithm and provide an example in Fig. 5(a) that has two iterations in the decoder. We see that the slot node e_5 receives a clean (i.e., not interfered) message from v_2 , which can then be decoded at the first step of the SIC procedure. We say that the edge (v_2, e_5) is revealed at the first iteration step and it can be removed from the graph, leading to a reduced graph. The decoded message from v_2 is then passed along the edge (v_2, e_3) to remove the interference at the third time slot of the MAC frame, namely e_3 . This means that the edge (v_2, e_3) is also revealed and removed from the graph. If at the i th iteration step of the decoding the message from the burst node v_3 has also been decoded (and so the message along (v_3, e_3) has been passed), the message from v_1 can be decoded through the slot node e_3 .

Dependencies between nodes in the graph can be described by a tree representation [24], which permits to study the iterative burst decoding process. Considering a burst node v , we are interested in the probability of decoding the message through a slot node e . The associated tree is the one describing the neighborhood of e . This tree is rooted at v , with e as only branch going out from v , while the node e has branches to the neighboring burst nodes excluding v , as shown in Fig. 5 for the (v_1, e_3) edge.

In more details, let denote by $T_{i,k}$ the constructed tree of depth $2i$ with a BN of class k (e.g., v_1) as a root. Each node at depth $2i, 2i-2, \dots, 2, 0$ are BNs (of class k for the root and of any class for the other depths value) while the nodes at depth $2i-1, 2i-3, \dots, 3, 1$ are SNs. Finally, the nodes at depth $2i, 2i-2, \dots, 2, 0$ are denoted by OR-nodes, while the nodes at depth $2i-1, 2i-3, \dots, 3, 1$ are AND-nodes in the tree representation. In the tree representation, a BN at depth $2i$ (a SN at depth $2i-1$) is marked with 1 if it is decoded (if it receives a clean message) at the i th iteration step, and marked with 0 otherwise. For the message sent from v_1 to be decoded at the i th decoding step through the slot node e_3 , the slot node e_3 has to be marked with 1. This happens *if all* the other $(l-1)$ neighboring BNs of e_3 are decoded or marked with 1 (AND-operator), where l is the degree of the slot node under consideration. We denote by z_i the probability of the slot nodes at depth $2i-1$ to be marked with 0. We consider now the probability that any BN of degree l at depth i in the tree is marked with 1. This happens *if at least one* of the remaining $(l-1)$ neighboring SNs is marked with 1, i.e., if it has a non-interfered message (OR-operator). We denote by $y_{i,k}$ the probability that the message along the considered edge is not decoded. In our IRSA scheme, the messages transmitted by the sources are not known a priori and they need to be decoded. This means that none of the BNs is known a priori before the decoding process starts, i.e., $y_{0,k} = 1, \forall k$ and $z_0 = 1$ and all leafs are initially marked with 0.

We now evaluate the probability of having a BN of class k unknown after the i th iteration of the decoding process. This is given by

$$y_{i,k} = P\{\text{all AND nodes at depth } 2i-1 \text{ are marked with 0}\} = \sum_{l=1}^{N-1} z_{i-1}^{l-1} \lambda_{l,k} = \lambda_k(z_{i-1}) \quad (15)$$

where z_{i-1} is the probability of having a AND-node at depth $2i-1$ that is marked with 0 and $\lambda_{l,k}$ is the probability for an edge to be incident to a degree- l BN of class k . Each child of a AND-node is a OR-node of class k with probability q_k , given by

$$q_k = \frac{L_k \Lambda'_k(1)}{\sum_{k=1}^K L_k \Lambda'_k(1)}$$

which is the ratio between the average number of edges going out from all BNs of class k , namely $L_k \Lambda'_k(1)$, and the average number of total edges in the graph, namely $\sum_{k=1}^K L_k \Lambda'_k(1)$. It follows that

$$z_{i-1} = 1 - P\{\text{all OR nodes at depth } 2i-2 \text{ are marked with 1}\} \quad (16a)$$

$$= 1 - \sum_{l=1}^{M-1} \left[1 - \underbrace{P\{\text{one OR node at depth } 2i-2 \text{ is marked with 0}\}}_{\sum_{k=1}^K q_k y_{i-1,k}} \right]^{l-1} \rho_l \quad (16b)$$

$$= 1 - \sum_{l=1}^{M-1} \left[1 - \sum_{k=1}^K q_k y_{i-1,k} \right]^{l-1} \rho_l \quad (16c)$$

$$= 1 - \rho \left(1 - \sum_{k=1}^K q_k y_{i-1,k} \right) \quad (16d)$$

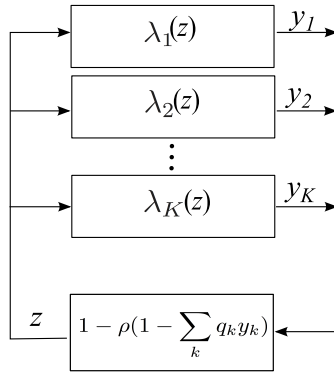


Figure 6. Feedback loop associated to the iterative decoding probability described in Eq. (17). Each error probability $y_{i,k}$ is evaluated as a function of the z_{i-1} , while z_{i-1} is evaluated as a function of a weighted sum of all $y_{i-1,k}$ probabilities. This recursion creates the feedback loop depicted in the figure.

where in Eq. (16b) the probability of having one OR node at depth $2i - 2$ marked with 0 is given by $\sum_{k=1}^K q_k y_{i-1,k}$. This corresponds to the probability of having a OR node at depth $2i - 2$ and of class k marked with 0, weighted by the probability of having a OR node of class k as child. Substituting Eq. (16d) into Eq. (15), we obtain the following recursion

$$\begin{aligned} y_{i,k} &= \lambda_k(z_{i-1}) \\ z_{i-1} &= 1 - \rho \left(1 - \sum_{k=1}^K q_k y_{i-1,k} \right) \end{aligned} \quad (17)$$

with $y_{0,k} = 1, \forall k, q_0 = 1$ ¹. Note that the error probability $y_{i,k}$ is recursively derived assuming that the OR nodes at depth $2i - 2$ are actually roots of trees with depth $2i - 2$ and are independent from each others. Substituting Eq. (14) into Eq. (17), we obtain

$$y_{i,k} = \lambda_k \left(1 - \exp \left(-G \frac{\sum_k L_k \Lambda'_k(1)}{\sum_k L_k} \sum_{k=1}^K q_k y_{i-1,k} \right) \right) \quad (18)$$

Finally, let $P_e(k, I)$ be the probability for the base station of not correctly decoding the message sent from a BN of class k when a iterative SIC technique is adopted with a maximum of I iterations. As already observed in Fig. 5, the message (BN) of class k can be decoded through any neighboring SN. It means that $P_e(k, I)$ is computed as the probability that the message cannot be decoded through any edge at the i th iteration of the SIC algorithm, which means that

$$P_e(k, I) = \sum_{l=0}^N y_{I,k}^l \Lambda_{l,k} \quad (19)$$

C. Stability Conditions

We are now interested in evaluating the conditions under which the SIC algorithm asymptotically ($i \rightarrow \infty$) converges with zero failure probability. We first observe that the iterative decoding process described in Eq. (17) can be seen as a feedback loop (Fig. 6) of which we can study the global stability, by deriving the conditions under which the system asymptotically converges to null error probability, i.e., to an equilibrium point $(\mathbf{y}^*, z^*) = (\mathbf{0}, 0)$, for any initial probability (\mathbf{y}, z) . The global stability can be guaranteed if the error probability z_i decreases at every decoding iteration, converging then to a zero error probability for $i \rightarrow \infty$.

We first note that the control equations that characterize the feedback system, as well as the iterative decoding probability of Eq. (17), are

$$\begin{aligned} z &= 1 - \rho \left(1 - \sum_k q_k y_k \right) \\ y_k &= \lambda_k(z) \end{aligned}$$

¹In the above analysis we have assume a tree ensemble representation, which implies that the bipartite graph is loop-free, since loops introduce correlation in the evolution of the message error probabilities. This is true for large networks.

Table II
CONSIDERED POLYNOMIAL DISTRIBUTIONS PER CLASS Λ_k .

Index	Label	Transmission Probability Distribution $\Lambda_k(x)$
1	$\Lambda^a(x)$	$0.5102x^2 + 0.4898x^4$
2	$\Lambda^b(x)$	$0.5631x^2 + 0.0436x^3 + 0.3933x^5$
3	$\Lambda^c(x)$	$0.5465x^2 + 0.1623x^3 + 0.2912x^6$
4	$\Lambda^d(x)$	$0.5x^2 + 0.28x^3 + 0.22x^8$
5	$\Lambda^e(x)$	$0.08x^3 + 0.14x^4 + 0.3x^5 + 0.17x^6 + 0.14x^7 + 0.17x^9$
6	$\Lambda^f(x)$	$0.4977x^2 + 0.2207x^3 + 0.0381x^4 + 0.0756x^5 + 0.0398x^6 + 0.0009x^7 + 0.0088x^8 + 0.0068x^9 + 0.0030x^{11} + 0.0429x^{14} + 0.0081x^{15} + 0.0576x^{16}$

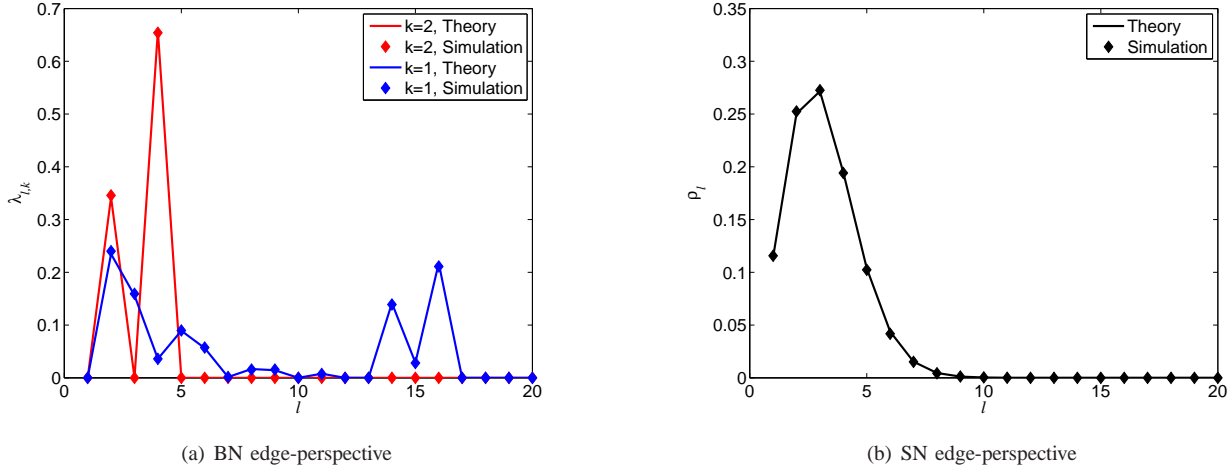


Figure 7. Comparison of the theoretical and simulated edge-perspective degree distributions for a system with $K = 2$, $N = 200$, $L_1 = L_2$, and $\Lambda_1(x) = \Lambda^f(x)$ and $\Lambda_2(x) = \Lambda^a(x)$.

as shown in Fig. 6. By substituting Eq. (14) in the above equations, we obtain the following control equation for the feedback system

$$z = 1 - \underbrace{\exp\left(-\frac{\sum_k L_k \Lambda'_k(1)}{N} \sum_{k=1}^K q_k \lambda_k(z)\right)}_{f(z)} \quad (20)$$

and we can guarantee global stability if $f(z) < z, \forall z$. This means that we should have

$$1 - \exp\left(-G \frac{\sum_k L_k \Lambda'_k(1)}{\sum_k L_k} \sum_{k=1}^K q_k \lambda_k(z)\right) < z. \quad (21)$$

In the following, we show how the global stability can be exploited to solve the transmission optimization problem in prioritized MAC algorithms.

D. Analytical Performance Validation

We now provide simulation results to validate the theoretical analysis provided above and study the performance of the random MAC transmission protocol in different settings. We set the maximum number of iterations used in the burst decoding algorithm to $I = 100$. For each simulated scenario, we average the experienced utility function over 1000 simulated loops. We test the theoretical analysis for different transmission probabilities, provided in Table II.

Fig. 7 first depicts the theoretical and simulated edge-perspective degree distribution for a scenario with $N = 200$ transmission slots in a MAC frame, $K = 2$ source classes with the same number of burst nodes (i.e., $L_1 = L_2$), and with the following degree distributions $\Lambda_1(x) = \Lambda^f(x)$ and $\Lambda_2(x) = \Lambda^a(x)$ that have been shown to be effective in random MAC strategies [9]. We see that the theoretical performance is in agreement with the simulation results, which means that the assumption of large networks used in the analysis still holds in the case of finite size of the MAC frame ($N = 200$), as observed in other works [9].

We further provide a comparison between simulations and theoretical results in terms of both normalized throughput and utility function. We consider an illustrative scenario with two classes with priority given by $w_1 = 0.7$ and $w_2 = 0.3$ (this means

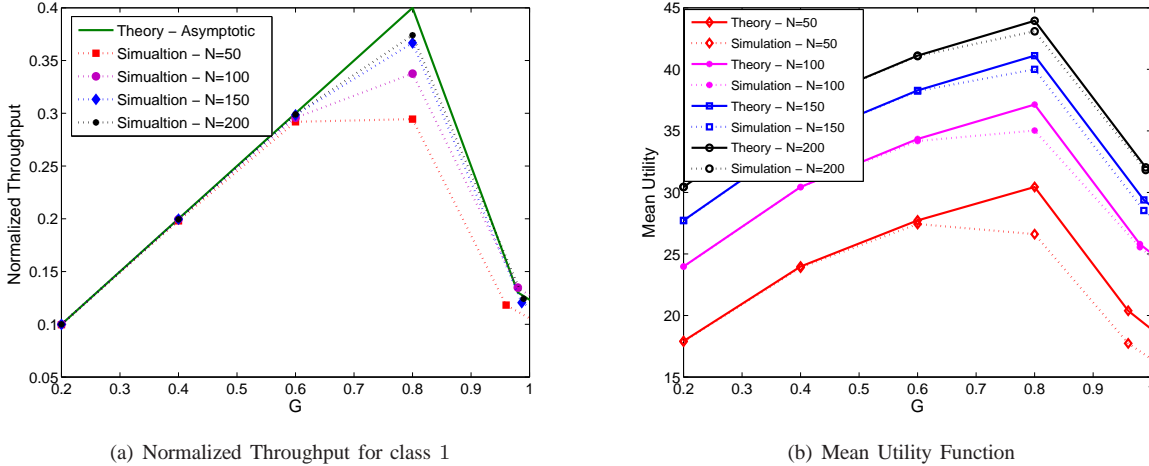


Figure 8. Heterogenous system performance vs. network load G for the case of $K = 2$, $w_1 = 0.7$, and $w_2 = 0.3$, $L_1 = L_2$, $\Lambda_1(x) = \Lambda^d(x)$ and $\Lambda_2(x) = \Lambda^a(x)$. Different numbers of transmission slots N are considered.

that class 1 is more important than class 2), with the same number of burst nodes $L_1 = L_2$, and two different distributions $\Lambda_1(x) = \Lambda^d(x)$ and $\Lambda_2(x) = \Lambda^a(x)$. In Fig. 8, both the average of the normalized throughput and the overall utility function are depicted as a function of the traffic load G for 1000 simulation runs, for different size of N of the MAC frame. The traffic load $G = \sum_k L_k/N$ varies with the number of burst slots $L_1 = L_2$, for a fixed N . The normalized throughput is evaluated as $G(1 - P_e(k, I))$, and we only show the throughput for class 1 since the results are mostly similar for all classes. We see that there is again a good match between theoretical and simulated results for all N larger than 50. When $N = 50$, the error in considering an asymptotic behavior is non negligible, but yet the utility function behavior is accurate. In particular, when $N = 50$, both theoretical and simulation values of the mean utility increases with G for $G < 0.6$, have a peak between $[0.6, 0.8]$, and decrease beyond a traffic value of 0.8. We have obtained similar trends in other experiments for different scenarios, and all confirm the validity of the analysis for large MAC frames and the possibility to characterize the optimal traffic load, even with small MAC frames.

We now illustrate the performance of prioritized transmission schemes for sources with different importance. In Fig. 9, the message error rate and the overall utility function are given as functions of the traffic load G for a sample scenario with $N = 200$ transmission slots, two classes with the same number of slots ($L_1 = L_2$) but with different priorities ($w_1 = 0.7$ and $w_2 = 0.3$). The traffic load $G = \sum_K L_K/N$ again varies with the number of burst nodes in each class. In order to illustrate the benefits of prioritized transmission when sources are heterogeneous, we compare the performance of equal and unequal transmission probabilities for different classes. For the equal transmission strategy, denoted by EEP, we consider $\Lambda_1(x) = \Lambda_2(x) = \Lambda^e(x)$; while for the case of unequal transmission strategy, denoted by UEP, we consider different distributions $\Lambda_1(x) = \Lambda^e(x)$ and $\Lambda_2(x) = \Lambda^b(x)$, which correspond to different transmission probabilities (namely higher replication rate for the most important classes). We first observe that theoretical results again match the simulations results computed over 1000 simulation runs. The results also show the benefit of prioritized transmission policies when source have different priorities. In Fig. 9(a), we see that the message error probability per class is higher for the EEP strategy than for prioritized strategy under consideration. We also observe that a EEP strategy leads to a waterfall effect in proximity of a threshold value of $G = 0.6$, while the UEP strategy has a larger threshold value of $G = 0.7$. A larger threshold value implies a larger throughput, since a larger number of sources actively transmit messages within a given MAC. This gain achieved by the UEP strategy is due to the change in the transmission protocol for different classes: in our example, the class 2 adopts a replication rate following $\Lambda_2(x)$ rather than $\Lambda_1(x)$, with a maximum node degree of 5 rather than 9. This reduces the overall number of messages sent in a MAC frame, hence also the load of the network. This reduced replication rate mainly affects class 2 rather than class 1, which is more important in our example. This leads to an overall utility function that reaches a maximum of 43.2 dB for the UEP strategy, as opposed to the maximum of 40.8 dB of the EEP strategy, see Fig. 9(b).

Another example of prioritized transmission is provided in Fig. 10, where the same scenario of Fig. 9 is considered, but with a different number of burst nodes in each class, i.e., $L_2 = \alpha L_1$, with $\alpha = 0.1$ and $\alpha = 0.33$. We see again that the theoretical and the simulation results are generally in accordance, especially in the low and high traffic regions. We further see that the number of burst nodes per class affects the performance of the prioritized transmission solution. In particular, reducing the number of burst in the lower importance class improves the overall system performance. Finally, we observe that theoretical study is an upper bound of the simulated performance and the theoretical value of G^* is an upper bound of the simulated value of G^* , where G^* the threshold value beyond which the error probability rapidly reaches 1 and a waterfall effect is experienced.

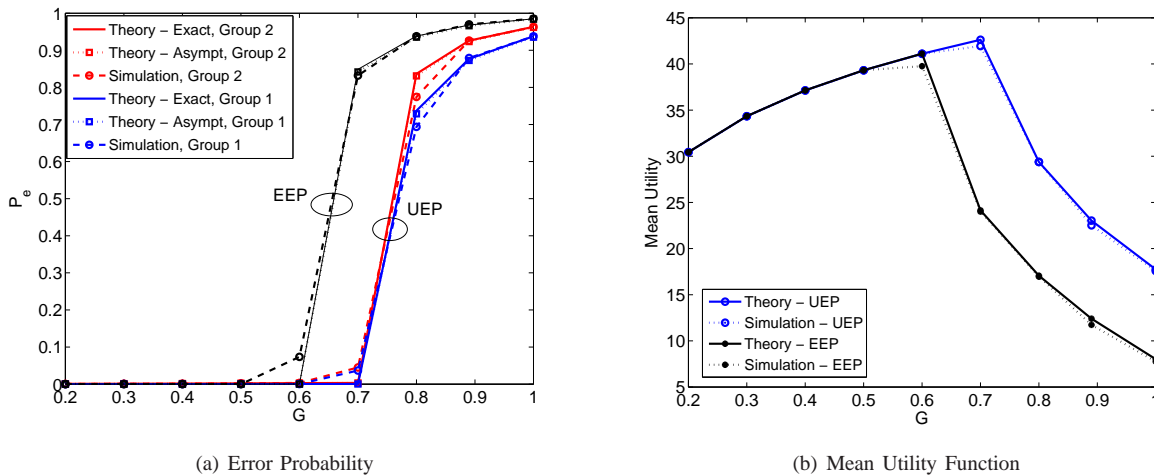


Figure 9. System performance vs. network load G for the case of $N = 200$, $K = 2$, $w_1 = 0.7$, and $w_2 = 0.3$, $L_1 = L_2$. For the UEP case $\Lambda_1(x) = \Lambda^e(x)$, and $\Lambda_2(x) = \Lambda^b(x)$ For the EEP case, $\Lambda_1(x) = \Lambda_2(x) = \Lambda^e(x)$.

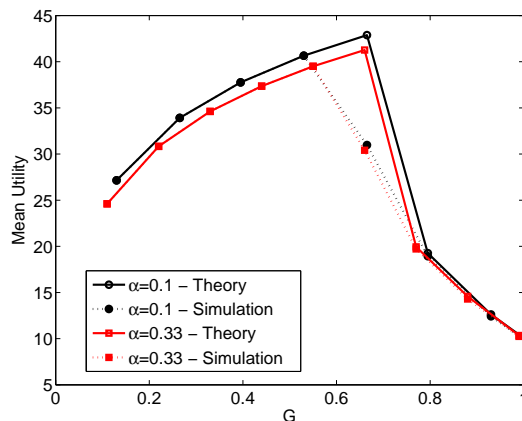


Figure 10. System performance vs. network load G for the case of UEP transmission, for $N = 200$, $K = 2$, $w_1 = 0.7$, and $w_2 = 0.3$, $L_2 = \alpha L_1$, $\Lambda_1(x) = \Lambda^e(x)$, and $\Lambda_2(x) = \Lambda^b(x)$.

Overall, the above results illustrate that prioritized transmission is beneficial when sources have different importance, and that the system performance is dependent on both the replication rates (or the transmission probabilities) and the number of burst nodes. In the following, we show how this theoretical study of MAC protocol strategies can be adopted in practical resource allocation optimization problems.

IV. PRIORITIZED RANDOM ACCESS OPTIMIZATION

Based on the above theoretical analysis, we formulate now a transmission policy optimization aimed at finding the best $(\Lambda_k(x), L_k)$ per class, such that the network resources are not under-utilized but not over-utilized either. More in details, we choose both the transmission probability and the source rate for each class, such that the overall system performance is maximized. The optimization, carried out by the base station, finds the best tradeoff between throughput and message decoding probability for the all sources.

A. Problem Formulation

Let denote by $\mathbf{\Lambda} = [\Lambda_1(x), \Lambda_2(x), \dots, \Lambda_K(x)]$ the transmission policy vector with the transmission probability distributions for each class. By varying $\mathbf{\Lambda}$ and the number of bursts L_k for source class k , we can actually modify the expected received throughput for each class. As the throughput corresponds to an utility function score for each class, as shown in Eq. (1), we can modify the overall system performance by tuning $\mathbf{\Lambda}$ and $\{L_k\}$. In particular, we can optimize the overall utility of a system with heterogenous sources by maximizing the throughput of most important classes and sacrificing the throughput of least important ones. This leads to prioritized transmission strategies that are necessary for systems with sources that have different

utility functions. Hence, instead of maximizing the overall throughput, we optimize the best transmission strategy $(\mathbf{\Lambda}, \mathbf{L})$ and select the one that maximizes the overall utility function, evaluated as follows

$$\begin{aligned} (\mathbf{\Lambda}^*, \mathbf{L}^*) &= \arg \max_{(\mathbf{\Lambda}, \mathbf{L})} \bar{U}(\mathbf{\Lambda}, \mathbf{L}) \\ &= \arg \max_{(\mathbf{\Lambda}, \mathbf{L})} \left\{ \sum_{R_1=0}^{L_1} \sum_{R_2=0}^{L_2} \dots \sum_{R_K=0}^{L_K} U(R_1, R_2, \dots, R_K) P_r^{(I)}(R_1, R_2, \dots, R_K; \mathbf{\Lambda}, \mathbf{L}) \right\} \end{aligned} \quad (22)$$

where $U(R_1, R_2, \dots, R_K)$ is the system utility function defined in Eq. (1) while $P_r^{(I)}(R_1, R_2, \dots, R_K; \mathbf{\Lambda}, \mathbf{L})$ is the probability of correctly receiving R_1, R_2, \dots, R_K messages for sources of class 1, 2, \dots , K , respectively. This corresponds to the probability of receiving R_1, R_2, \dots, R_K messages either with no collisions or messages with collisions that can be resolved with the iterative message recovering strategies (i.e., SIC) after a maximum number of I iterations.

Since the transmission processes are handled independently by all sources, we can derive the probability of correctly receiving the the messages from different sources as follows

$$\begin{aligned} P_r^{(I)}(R_1, R_2, \dots, R_K; \mathbf{\Lambda}, \mathbf{L}) &= \prod_{k=1}^K P_k^{(I)}(R_k; \Lambda_k(x), L_k) \\ &= \prod_{k=1}^K \binom{L_k}{R_k} [1 - P_e(k, I)]^{R_k} P_e(k, I)^{L_k - R_k} \end{aligned} \quad (23)$$

where $P_k^{(I)}(R_k; \Lambda_k(x), L_k)$ is the probability for a source of class k to recover R_k out of L_k messages after the I -th IC iteration, and $1 - P_e(k, I)$ is the probability for the base station to correctly receive the message sent from a source of class k . We can then express the expected distortion as

$$\bar{U}(\mathbf{\Lambda}, \mathbf{L}) = \sum_{R_1=0}^{L_1} \sum_{R_2=0}^{L_2} \dots \sum_{R_K=0}^{L_K} \sum_{k=1}^K w_k U_k(R_k) \prod_{R_K=0}^{L_K} \binom{L_k}{R_k} [1 - P_e(k, I)]^{R_k} P_e(k, I)^{L_k - R_k}. \quad (24)$$

and the problem formulation to be solved becomes

$$(\mathbf{\Lambda}^*, \mathbf{L}^*) : \arg \max_{\mathbf{\Lambda}, \mathbf{L}} \bar{U}(\mathbf{\Lambda}, \mathbf{L}) \quad (25a)$$

$$\text{s.t. } \Lambda_k(x) \leq \Lambda_{k+1}(x) \quad \forall x \in [0, 1], \forall k \quad (25b)$$

where the priority constraint in Eq. (25b) permits to reduce the search space. In particular, we constraint the optimization to an unequal recovery probability among classes such that sources from more important classes have a larger probability of correctly transmitting their messages compared to lower important sources. This translates in imposing $P_e(k, i) \leq P_e(k+1, i)$ for class k more important than class $k+1$. From Eq. (19), the priority condition can be generalized as $\Lambda_k(y_{i-1, k}) \leq \Lambda_{k+1}(y_{i-1, k+1})$. The optimization problem in Eq. (25) results in maximizing the overall system utility.

B. Approximated Solution

The optimization problem in Eq. (25) might not be easily solved with conventional optimization frameworks. The expected utility function is evaluated as a weighted sum of binomial distributions, each of them having a probability $P_e(k, I)$. Although $P_e(k, I)$ can be considered as a sigmoid function to simplify the formulation, there is no a convenient optimization framework that is able to address the above problem jointly for both $\mathbf{\Lambda}$ and \mathbf{L} variables, to the best of our knowledge. Thus, we propose a solving method that exploits an intrinsic property of the coded slotted ALOHA: the message error probability usually follows a waterfall effect [25], having an error probability approaching 0 for traffic network G lower than a given threshold G^* , and rapidly approaching 1 beyond G^* . The threshold value G^* is usually defined as the value that is the limit of the region where the condition of stability hold.

In the following, we approximate the message error probability $P_e(k, I)$ to 0 when the stability condition is respected, i.e., when the convergency of the iterative message decoding algorithm is assumed. By imposing the global stability condition of Eq. (21), we have the following instance of the optimization problem:

$$(\mathbf{\Lambda}^*, \mathbf{L}^*) : \arg \max_{\mathbf{\Lambda}, \mathbf{L}} \sum_{k=1}^K w_k U(L_k) \quad (26a)$$

$$\text{s.t. } \Lambda_k(x) \leq \Lambda_{k+1}(x) \quad \forall x \in [0, 1], \forall k \quad (26b)$$

$$\exp \left(-G \frac{\sum_k L_k \Lambda'_k(1)}{\sum_k L_k} \sum_{k=1}^K q_k \lambda_k(x) \right) > 1 - x \quad \forall x \in [0, 1]. \quad (26c)$$

Algorithm 1 Prioritized Random Access Protocol Optimization

1: **step 1**): Define the set \mathcal{L}_{ON} defined as the set of pairs $(\mathbf{\Lambda}, \mathbf{L})$ in the ON region:

$$\mathcal{L}_{\text{ON}} : \{(\mathbf{\Lambda}, \mathbf{L}) \text{ s.t. the constraint in Eq. (26c) is verified}\}$$

2: **step 2**): Optimize the utility function within the ON region as follows

$$\begin{aligned}
 (\mathbf{\Lambda}^*, \mathbf{L}^*) : \arg \max_{(\mathbf{\Lambda}, \mathbf{L}) \in \mathcal{L}_{\text{ON}}} & \sum_{k=1}^K w_k U(L_k) \\
 \text{s.t. } & \Lambda_k(x) \leq \Lambda_{k+1}(x) \quad \forall x \in [0, 1], \forall k
 \end{aligned}$$

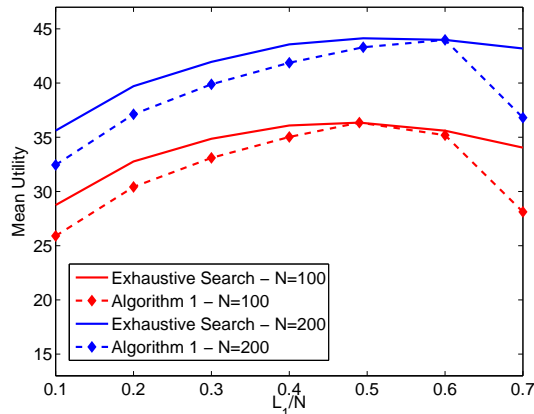


Figure 11. Optimized system performance vs L_1 for the case of $\Lambda_1(x) = \Lambda_2(x) = \Lambda^e(x)$. The best value of L_2 is optimized for each value L_1 .

where we have assumed a null error probability if the constraint in Eq. (26c) is met for all classes, i.e., if the conditions for global stability are met. This means that the L_k messages sent from sources of class k are correctly received. The experienced utility function in each class is therefore $U_k(L_k)$, and the global utility is the weighted sum of class utilities.

In the following, we denote by *ON region* the set of pairs of $(\mathbf{\Lambda}, \mathbf{L})$ such that the stability condition is respected. The above optimization problem permits to select the ON region of the system and to seek for a solution within the region where all packets are decoded. This instance of our optimization problem in Eq. (25) offers simpler solution to the selection of the best transmission strategy.

The optimization problem can be easily solved in two steps, as described in Algorithm 1. The first step (Step 1) defines the boundaries of the ON region by simply solving Eq. (26c), for the global stability. Then, finding the best pair $(\mathbf{\Lambda}^*, \mathbf{L}^*)$ in the ON region reduces to solving the optimization in Step 2. This optimization has an objective function that has the form of a weighted sum of utility functions subject to K affine constraints. Thus, it can be easily solved for concave or linear $U(L_k)$ by concave or linear programming optimization, or by more general gradient-based optimization methods for more general non-decreasing utility functions $U(L_k)$.

C. Simulation Results

We now provide simulation results to study the performance of the prioritized random MAC transmission protocol in different settings. We set the maximum number of iterations used in the burst decoding algorithm to $I = 100$. For each simulated scenario, we average the experienced utility function over 1000 simulated loops. As utility function, we consider $U_k(R_k) = \log(R_k)$, $\forall k$, which resembles a typical image quality metric. In Section III-D, we have shown that the theoretical study of Section III-B is an upper bound of the simulated performance and the theoretical value of G^* is an upper bound of the simulated value of G^* , where G^* is the end of the ON region where the error probability is negligible. While the asymptotic theoretical bound is surely good to design reliable replication rates $\Lambda(x)$, it might lead to approximate solutions for the optimization of the resource allocation \mathbf{L} in finite MAC size. In the following, first we show the main limitations of the optimization method based purely on the theoretical study. Then, we describe how these bounds combined with well-chosen heuristics can be adopted to jointly optimize $(\mathbf{\Lambda}, \mathbf{L})$ for selecting effective prioritized transmission strategies and we show that the proposed approximated algorithm still achieves performance that is close to the optimal one.

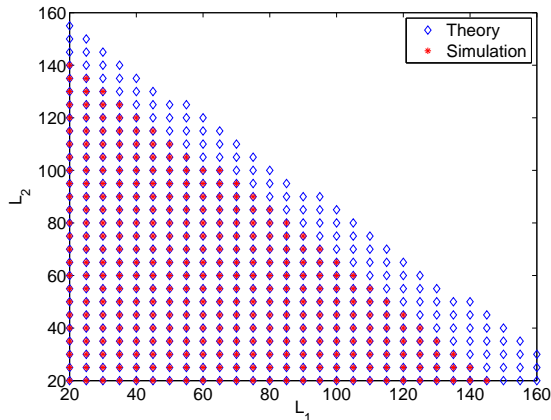


Figure 12. Example of ON region for a system with two source classes, $N = 200$, $\Lambda_1(x) = \Lambda^e(x)$, and $\Lambda_2(x) = \Lambda^a(x)$.

We first study the optimization of the number of burst nodes per class. In Fig. 11, we show the global utility function as a function of the number of burst nodes in class 1 (namely, L_1 normalized by N), for the case of two source classes, with different importance $w_1 = 0.7$, $w_2 = 0.3$, identical transmission probability distributions $\Lambda_1(x) = \Lambda_2(x)$, and $N = 100$ or 200 . For each value of L_1 , we evaluate the best value of L_2 and plot the corresponding global utility score. The Algorithm 1 is considered for the optimization, where the global stability condition has been imposed by Eq. (26c) in the first step of the optimization algorithm. These results are compared with simulations results where the optimal L_2 for each L_1 is found by exhaustive search. For both $N = 100$ and $N = 200$, we notice that the global stability condition imposes a stringent condition, leading to a tight bound of the ON region compared to the simulated one. This leads to a mean utility score that is almost as good as the optimal one. However, we notice that the model is not highly reliable for large values of L_1 . For example, for $L_1/N = 0.7$ in both cases of $N = 100$ or 200 slots, the theoretical optimization leads to a substantial drop in the utility function. This drop is due to the mismatch between theoretical and simulation results around G^* , as discussed in Section III-D.

We now better study the effect of the mismatch between theoretical stability conditions and actual ones in the optimization algorithm. We recall that the ON region is the one that satisfies the global stability in Eq. (26c). We show in Fig. 12 the ON region for a case with $K = 2$ classes, $N = 200$ transmission slots, and the transmission probability distributions are $\Lambda_1(x) = \Lambda^e(x)$, and $\Lambda_2(x) = \Lambda^a(x)$. The ON region boundaries are derived as a function of the number of burst nodes (or equivalently the traffic) both from simulations and from the theoretical analysis through the global stability condition of Eq. (20). In the simulations we evaluate the ON region as the one where the decoding error probability after SIC is lower than 10^{-4} . As expected, the theory gives an ON region (in blu diamonds) that is more extended than the actual one (red points), since the theoretical ON region gives an upper bound on the value of traffic G^* that represents the transition between ON and OFF regions of the SIC algorithm. Unfortunately, the best L derived from Algorithm 1 approaches the boundary of the ON region defined by theoretical stability conditions, which is exactly the unsafe region where the theory does not necessary match the actual behavior of the system. This means that for most cases, the optimization of Algorithm 1 would select a transmission strategy such that the network is actually overloaded, which results in a poor mean utility function. Based on these observations, we can actually overcome the main limitation of the theoretical study with the effective following heuristics.

The key concept is that we would like the system to work *almost* at the boundaries of the ON region, but not *exactly* at the boundaries. A first solution is to use the theoretical study to evaluate the boundaries, and then run simulations in a neighborhood of the boundaries to predict the actual ON region. This method is however not always feasible because of the computational complexity in simulating the considered scenario. However, for all the scenarios considered in our work, we empirically observe that the theoretical ON region extends beyond the actual one by about $0.1G$. Thus, a good heuristic solution, called Algorithm 2, consists in first evaluating the theoretical bound on the ON region and then translating into a “safe boundary” by reducing the boundaries by 10%. Finally, we can seek for the best (\mathbf{A}, \mathbf{L}) within the safe boundary region only, where the decoding error probability is actually zero. It is worth noting that the best (\mathbf{A}, \mathbf{L}) is selected as the best resource allocation \mathbf{L} such that the utility function is maximized and (\mathbf{A}, \mathbf{L}) is on the *actual* ON region boundaries. Note that it is much better to work with a traffic load that is slightly lower than the optimal one G^* , rather than working at a traffic load slightly larger than G^* . Working beyond the actual ON boundaries leads to a state of error probability that is quickly approaching 1, such that the achieved throughput can quickly fall to zero. In the following, we illustrate this statement by comparing the performance of Algorithm 1 and Algorithm 2.

We propose now experiments where we compare the performance of Algorithm 1 and Algorithm 2. To evaluate the set of pairs (\mathbf{L}, \mathbf{A}) that satisfies the stability constraints in the first step of both Algorithms, Eq. (26c) can be solved for example by differential evolution [26] as shown in [9]. The best polynomial distribution can also be evaluated by numerical analysis by

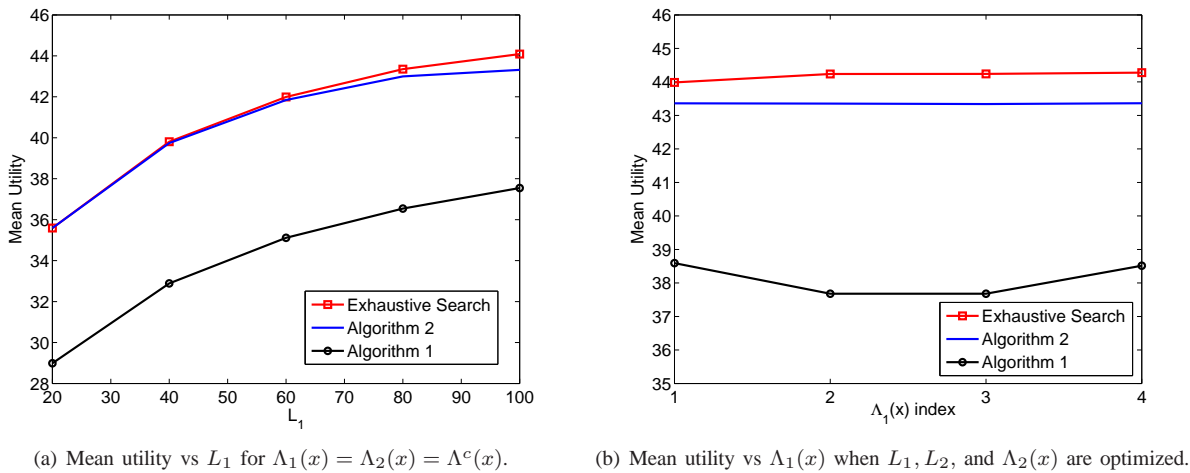


Figure 13. Optimization performance for Algorithm 1 and Algorithm 2 for a system with $N = 200$, and source importance given as $(w_1, w_2) = (0.7, 0.3)$.

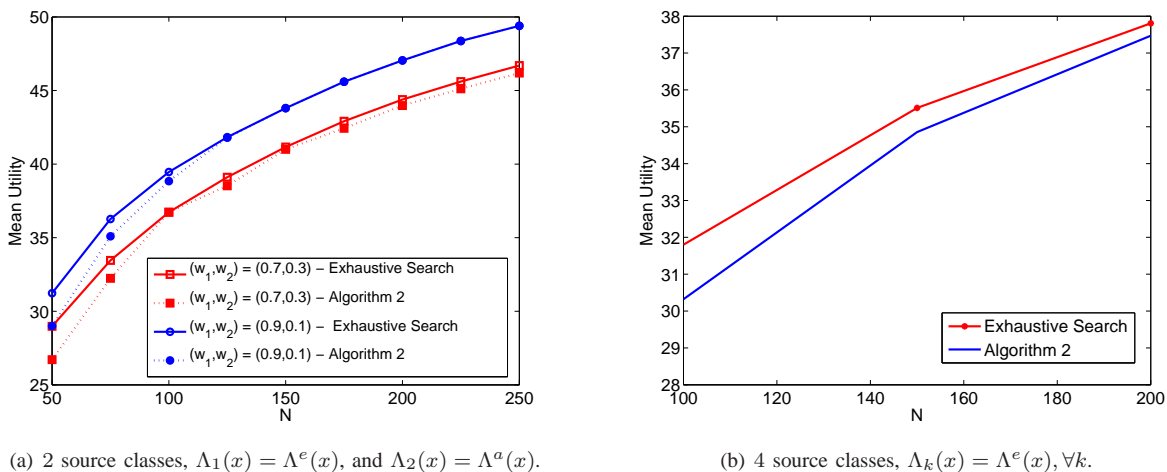


Figure 14. Mean utility vs. the MAC frame size N , when $\{L_k\}$ is optimized in the case of 2 and 4 source classes.

fixing a maximal degree for the BNs [27]. However, for the sake of simplicity, in the following we consider the polynomial distributions $\Lambda_k(x)$ derived from [9] and provided in Table II, which have been optimized to maximize the traffic threshold G^* . Any distribution in the table is a candidate for being assigned as transmission strategy to a given source class. However, our optimization can be applied to any other sets of polynomial distributions that satisfies Eq. (26c). We compare the performance of both algorithms to an exhaustive search through all $(\mathbf{L}, \mathbf{\Lambda})$ possible pairs, which leads to optimal performance in our scenario. For the sake of clarity, we show the results of our joint optimization over \mathbf{L} and $\mathbf{\Lambda}$ as functions of one parameter at time.

Fig. 13(a) depicts the mean utility function as a function of the number of burst slots in the first class L_1 , for $\Lambda_1(x) = \Lambda_2(x) = \Lambda^c(x)$, $N = 200$ transmission slots, and source importance $(w_1, w_2) = (0.7, 0.3)$. For each value of L_1 , the number of messages in the second class L_2 is optimized with the different algorithms. Analogously, in Fig. 13(b), the optimal utility function is depicted for different polynomial distributions $\Lambda_1(x)$, where the indexes on the x-axis follow the order in Table II. For each distribution $\Lambda_1(x)$, $\Lambda_2(x)$ and (L_1, L_2) are optimized with the algorithms under comparison. For both figures, the optimization based on the theoretical ON region does not match the optimal results achieved by exhaustive search. This is due to the mismatch between theoretical and actual ON region, as described above. However, we can observe that the optimization based on the safe ON region in Algorithm 2 achieves a performance that approaches the optimal one. We also observe that by increasing the number of BNs dedicated to the most important class (i.e., L_1) the global utility function increases (Fig. 13(a)). This is expected since a more prioritized transmission strategy is offered for large values of L_1 . If we rather look at the evolution of the global utility function as a function of several transmission probability distributions in Fig. 13(b), we notice an almost constant behavior. This is justified by the fact that the MAC frame can be efficiently utilized and by properly tuning $\Lambda_2(x)$, L_1 , and L_2 for each value of $\Lambda_1(x)$, the system achieves a large enough throughput to be in the floor region of the logarithmic utility function.

We further evaluate the performance of the optimization method proposed in Algorithm 2 in different system settings and provide in Fig. 14(a) the mean utility function as a function of the number of transmission slots N , given that two classes are considered with $\Lambda_1(x) = \Lambda^e(x)$, and $\Lambda_2(x) = \Lambda^a(x)$. The optimization consists in finding the best pair (L_1, L_2) for each value of N , for two different pairs of weight (w_1, w_2) . The optimal performance obtained via exhaustive search is compared to the one obtained with Algorithm 2. In all cases, we see that the Algorithm 2 reaches mean utility scores that are almost optimal. As expected, we also observe that the global utility function increases with N . Finally, we run experiments in a larger system with $K = 4$ classes with importance $(w_1, w_2, w_3, w_4) = (0.6, 0.2, 0.1, 0.1)$. The overall utility function is again provided as a function of the MAC frame size N when the number of messages is optimized with Algorithm 2 and Exhaustive search. The polynomial distribution is set to $\Lambda_k(x) = \Lambda^e(x)$ for all $k = [1, 4]$. The results in Fig. 14(b) confirm the good match of the performance of our heuristic-based optimization algorithm with the optimal performance. We notice again that the achieved overall utility function increases with the MAC frame size N , as expected.

In conclusion, we have shown that the SIC theory can be applied to practical optimization problems, namely resource allocation strategies for prioritized sources. An optimal resource allocation should be evaluated either by finite-length analysis (which is unfortunately not available in the literature for IRSA cases) or by simulation results (not feasible in terms of computational complexity). Thus, we have proposed an effective heuristic solution that is practical to use and achieves performance approaching the optimal one.

V. CONCLUSIONS

We have proposed prioritized new IRSA transmission strategies for systems with sources with different levels of importance. We have derived a theoretical study of the system performance in IRSA schemes with heterogenous sources and analyzed the asymptotic message error probability per class, as well as the global stability conditions. We have then proposed a new optimization problem aimed at finding the best transmission strategy in prioritized IRSA, in terms of both the replication probability and the source rate per class. A carefully designed heuristic-based algorithm has also been developed in order to optimize the transmission strategy in realistic conditions. Simulation results have validated our theoretical analysis and demonstrated the gain of the proposed prioritized strategy. The proposed solution is practical and yet accurate, achieving performance close to the optimal one. This work provides the main theoretical and practical tools for a system designer to optimally select transmission strategies for prioritized sources communicating to a common base station in an uncoordinated way.

REFERENCES

- [1] A. Zanella, M. Zorzi, A. dos Santos, P. Popovski, N. Pratas, C. Stefanovic, A. Dekorsy, C. Bockelmann, B. Busropan, and T. Norp, "M2M massive wireless access: Challenges, research issues, and ways forward," in *Proc. IEEE Globecom Workshops*, Dec 2013, pp. 151–156.
- [2] J. G. Andrews, S. Buzzi, W. Choi, S. V. Hanly, A. E. Lozano, A. C. K. Soong, and J. C. Zhang, "What will 5g be?" *ArXiv*, vol. /1405.2957, 2014.
- [3] J. Wu and G. Y. Li, "Collision-tolerant media access control with on-off accumulative transmission," *IEEE Trans. Wireless Commun.*, vol. 12, no. 1, pp. 50–59, 2013.
- [4] G. Cocco, N. Alagha, C. Ibars, and S. Cioni, "Network-coded diversity protocol for collision recovery in slotted aloha networks," *International Journal of Satellite Communications and Networking*, vol. 32, no. 3, pp. 225–241, 2014.
- [5] G. Cocco, S. Pfletschinger, and M. Navarro, "Seek and decode: Random access with physical-layer network coding and multiuser detection," *ArXiv*, vol. 1406.4736, 2014.
- [6] E. Casini, R. De Gaudenzi, and O. Herrero, "Contention resolution diversity slotted ALOHA (CRDSA): An enhanced random access scheme for satellite access packet networks," *IEEE Trans. on Wireless Commun.*, vol. 6, no. 4, pp. 1408–1419, 2007.
- [7] Y. Yu and G. Giannakis, "High-throughput random access using successive interference cancellation in a tree algorithm," *IEEE Trans. Inform. Theory*, vol. 53, no. 12, pp. 4628–4639, 2007.
- [8] S. Andreev, E. Pustovalov, and A. Turlikov, "Analysis of robust collision resolution algorithm with successive interference cancellation and bursty arrivals," in *Proc. Intern. Conf. on ITS Telecommunications (ITST)*, 2011, pp. 773–778.
- [9] G. Liva, "Graph-based analysis and optimization of contention resolution diversity slotted ALOHA," *IEEE Trans. Commun.*, vol. 59, no. 2, pp. 477–487, 2011.
- [10] E. Paolini, G. Liva, and M. Chiani, "Coded slotted ALOHA: A graph-based method for uncoordinated multiple access," *ArXiv*, vol. /1401.1626, 2014.
- [11] C. Stefanovic, P. Popovski, and D. Vukobratovic, "Frameless ALOHA protocol for wireless networks," *IEEE Commun. Lett.*, vol. 16, no. 12, pp. 2087–2090, 2012.
- [12] C. Stefanovic and P. Popovski, "Aloha random access that operates as a rateless code," *IEEE Trans. Commun.*, vol. 61, no. 11, pp. 4653–4662, November 2013.
- [13] E. Paolini, C. Stefanovic, G. Liva, and P. Popovski, "Coded random access: How coding theory helps to build random access protocols," *ArXiv*, vol. 1405.4127, 2014.
- [14] "IEEE ICC 2014 workshop on massive uncoordinated access protocols," 2014. [Online]. Available: <http://www.massap.org>
- [15] A. Munari, M. Heindlmaier, G. Liva, and M. Berlioli, "The throughput of slotted aloha with diversity," *ArXiv*, vol. 1401.3660, 2014.
- [16] C. Stefanovic, M. Momoda, and P. Popovski, "Exploiting capture effect in frameless ALOHA for massive wireless random access," *ArXiv*, vol. 1401.1714, 2014.
- [17] N. Rahnavard, B. Vellambi, and F. Fekri, "Rateless codes with unequal error protection property," *IEEE Trans. Inform. Theory*, vol. 53, no. 4, pp. 1521–1532, 2007.
- [18] D. Sejdinovic, D. Vukobratovic, A. Doufexi, V. Senk, and R. Piechocki, "Expanding window fountain codes for unequal error protection," *IEEE Trans. Commun.*, vol. 57, no. 9, pp. 2510–2516, 2009.
- [19] S. Sandberg and N. von Deetzen, "Design of bandwidth-efficient unequal error protection ldpc codes," *IEEE Trans. Commun.*, vol. 58, no. 3, pp. 802–811, March 2010.
- [20] Y. H. Wang, "On the number of successes in independent trials," *Statistica Sinica*, vol. 3, no. 2, pp. 295–312, 1993.

- [21] M. Fernandez and S. Williams, "Closed-form expression for the poisson-binomial probability density function," *IEEE Trans. on Aerospace and Electronic Systems*, vol. 46, no. 2, pp. 803–817, April 2010.
- [22] Y. Hong, "On computing the distribution function for the poisson binomial distribution," *Computational Statistics & Data Analysis*, vol. 59, pp. 41–51, 2013.
- [23] J. L. Hodges and L. Le Cam, "The poisson approximation to the poisson binomial distribution," *The Annals of Mathematical Statistics*, pp. 737–740, 1960.
- [24] M. G. Luby, M. Mitzenmacher, and M. A. Shokrollahi, "Analysis of random processes via and-or tree evaluation," in *Proceedings of the Ninth Annual ACM-SIAM Symposium on Discrete Algorithms*, 1998.
- [25] T. Richardson and R. Urbanke, *Modern coding theory*. Cambridge University Press, 2008.
- [26] R. Storn and K. Price, "Differential evolution a simple and efficient heuristic for global optimization over continuous spaces," *Journal of Global Optimization*, vol. 11, no. 4, pp. 341–359, 1997.
- [27] D. Jakovetic, D. Bajovic, D. Vukobratovic, and V. S. Crnojevic, "Cooperative slotted Aloha for multi-base station systems," *ArXiv*, vol. /1407.1109, 2014. [Online]. Available: <http://arxiv.org/abs/1407.1109>